Image-guided tomography: structure conforming inversion for complex overburden

Guy Hilburn[1*], Yang He[1], Francis Sherrill[1], Taejong Kim[1] and Zengjia Yan[1] present a high-resolution tomography method which flattens gathers reliably and quickly, while yielding geologically plausible velocity models.

Traditional methods of updating velocity models by seismic tomography rely on a number of assumptions and simplifications. In many situations, these may either increase the amount of time or number of tomographic iterations required to flatten events in migration gathers, or even make gathers worse. In other cases, the velocity models obtained with these techniques may turn out to be physically unlikely, as they do not rely on prior geological knowledge. We have developed a high-resolution tomography method called image-guided tomography (IGT), which is composed of two key ingredients: inversion preconditioned by image-guided interpolation (IGI) and an offset-dependent residual moveout (RMO) picking technique. IGT flattens gathers more reliably and quickly than traditional methods, while yielding more geologically plausible velocity models.

Traditional tomographic inversion can usually yield reasonable velocity updates which can flatten gathers within an acceptable range, but results may not follow any geologically-consistent pattern. Without restriction, velocities often violate layering and faults in an implausible manner. In addition, the best option to obtain the highest resolution inversion results previously was to use as fine an update grid as possible. This was computationally impractical and still tended to yield updates which needed smoothing to remove strong variations and outlying values. Hale (2009a) proposes using IGI to describe an image with a sparse set of values which are interpolated along structures, and suggests possibilities for restricting seismic imaging processes. Our edge-preserving image-guided tomography applies IGI preconditioning within inversion to automatically encourage velocity updates to honour layering and faults, leading to more believable subsurface models.

Mainstream RMO picking methods fall into two major categories (Woodward et al., 2008). In the first, polynomial-based techniques approximate moveout by fitting events to a parabola, hyperbola, or higher order polynomial curve. As a more recent alternative, offset-dependent methods pick moveout independently across numerous offsets. When implemented, offset-dependent picking may flatten gathers more accurately, and in fewer tomographic iterations, than polynomial-based methods.

Either of these methods allows the creation of higher-resolution velocity models than traditional techniques, and combining them can further their capabilities. When inversion updates are restricted to follow image-related structures, results can be attained more rapidly, and do not need the same post-processing which may create low resolution updates from even the densest inversions. Tracking and considering complex moveout with offset-dependent picking leads directly to more complex and appropriately variable velocity updates, and can even speed up the tomographic process.

Image-guided inversion

The structure-oriented IGT method relies on calculating several parameters from the most recent stacked image, which are then used to condition the inversion results to enforce their conformance to the underlying geology (Hale, 2009a).

By grouping all grid points into a small number of zones, we can limit the number of unknowns within the inversion process, effectively stabilizing the inversion based on our prior information. Therefore, our technique is initialized by selecting a grid of sparse control points, used to define an array of zones covering the update region. In order to enforce the constraint that these zones follow the underlying seismic image used to guide this process, we define their boundaries automatically based on structure-related propagation time within that image. A set of tensors is calculated from localized image gradients to describe the directionality and continuity of reflectors. The structure-related propagation time is then determined by solving the Eikonal equation as we move away from each control point, based on the structure tensors. Propagation time is lower along coherent structures, such as clearly-defined layers, and propagation time is higher across or against coherent structures or at disruptions in the image, such as faults. Each control point is then assigned to the zone of grid locations nearest to it in propagation time. These zones will therefore be anisotropic and extended along coherent structures, and will tend to

[1] *TGS.*

[*] *Corresponding Author, E-mail: Guy.Hilburn@tgs.com*

be more isotropic in incoherent areas, or when interrupted by faults. This method will automatically create edge-preserving zones which will tend to stop at faults yet will be able to resolve thin layers and small velocity anomalies when these are reflected in the stacked image.

During tomographic inversion, a matrix of equations is solved to find a velocity update which converges to a solution to minimize RMO. The basic relations governing this are

$$Am = d \text{ and } Lm = 0, \tag{1}$$

where m represents the model parameters such as velocity, d is the data term given by the RMO, A is the sensitivity matrix which determines the relationship between the current model and data, usually obtained from ray tracing, and L is the regularization operator used to stabilize the inversion. The objective is to iteratively update our model, given the RMO, which represents the inaccuracy in the current model. This process continues until the residual data misfit falls below a certain threshold.

In IGT, the first of the two relations in equation (1) is modified to

$$Apx = d, \tag{2}$$

by replacing m with px. Here p represents the preconditioning IGI matrix. This is applied during each iteration in the inversion by averaging all values within each zone, and then performing structure-oriented smoothing (Hale, 2009b), using the previously-calculated structure tensors. This enforces the update's resemblance to the base image by smoothing features preferentially in the direction indicated by the tensors.

To ensure our approach is as consistent as possible, we have adapted a priority-based selection process to choose optimal control point placement automatically, rather than based on constant or smoothly-varying spacing. This method

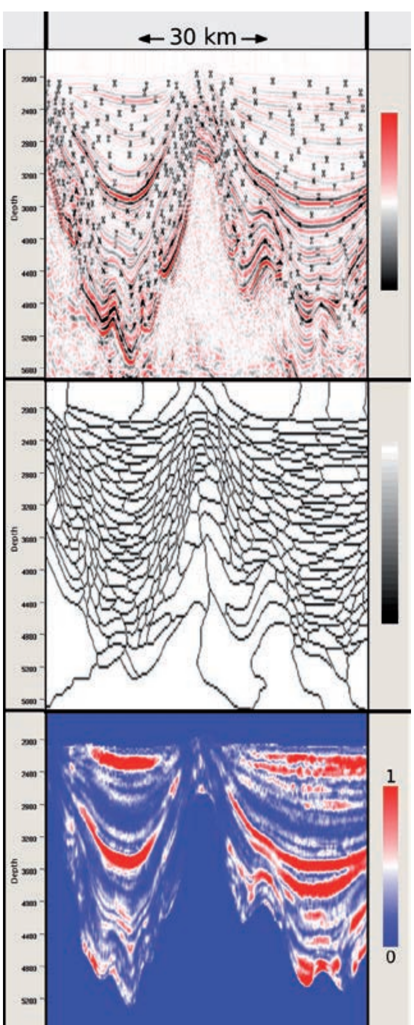

Figure 1 Angola example. (Top panel) adaptively-selected control points overlaid on the image used to guide interpolation in the update; (center panel) the boundaries of the selected update zones; (bottom panel) the priority map used to pick control points.

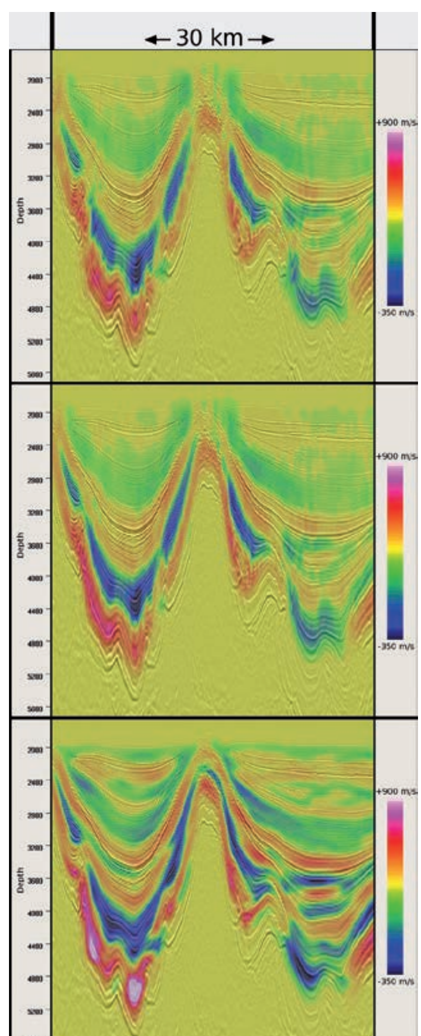

Figure 2 Angola example. Velocity update following inversion, overlaid on a migrated image, for: (top panel) traditional hyperbolic tomography with normal Laplacian regularization, (centre panel) hyperbolic tomography with dip-oriented Laplacian regularization, and (bottom panel) image-guided tomography.

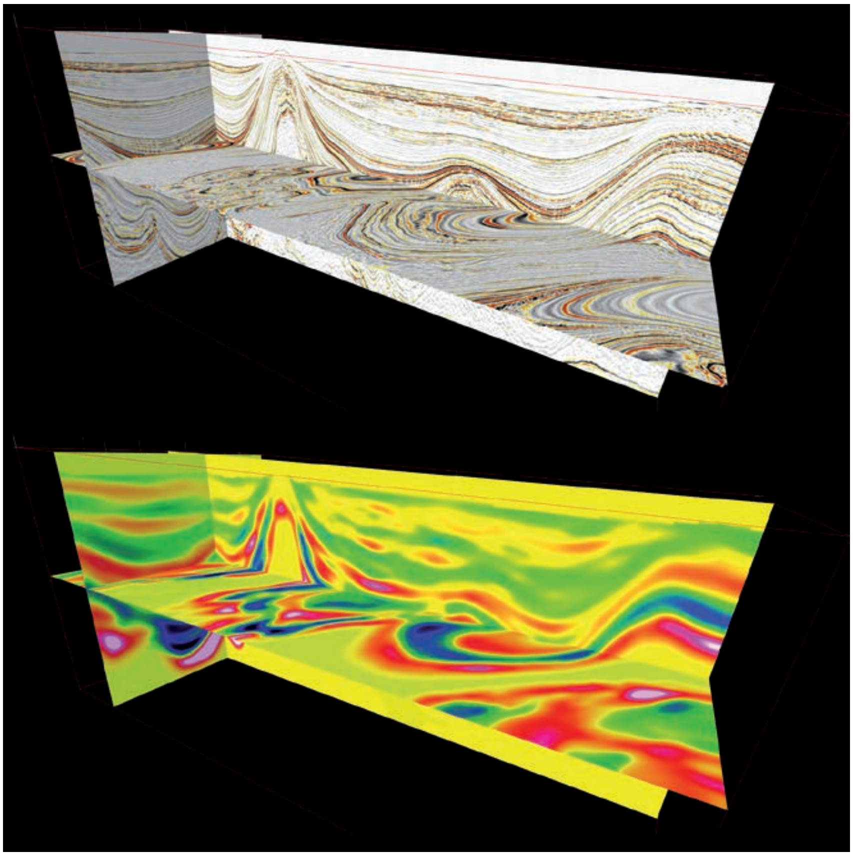

Figure 3 *Angola example. (Top panel) stacked image used to guide tomographic velocity updates; (bottom panel) velocity update derived using IGT, displaying strong correspondence to the underlying structures in all three directions, particularly for sharply dipping layers.*

was described by Cullison (2011) as an effective technique for selecting high-priority common image points for quality control checking, but it is useful in a variety of applications which require choosing important points within an image. In general, coherent structures need fewer control points which are spaced farther apart, as their properties will be more consistent along their length, while in incoherent areas, control points should be more closely spaced. Our adaptive method ranks locations based on importance, by building a priority map of the image by multiplying its amplitude envelope, structure-oriented semblance, and local planarity, which is represented by the level of anisotropy in the structure tensors. Control points are then picked in order of priority, while building exclusion zones around each to prevent points from being too close together in coherent regions.

Image-guided inversion example

In order to best demonstrate the capabilities of the IGT process, the method was applied over an area of an Angola dataset which shows ordered layering, areas of incoherent signal, and strongly dipping sediment, with the results shown in Figures 1,2 and 3.

Our adaptive control point selection process is demonstrated in Figure 1. Each 'x' in the top panel represents a control point chosen by picking locations of high value in the priority map shown in the bottom panel. Zones of high priority are usually found around strong, continuous reflectors, where the image has a high degree of coherence. Control points tend to be spaced far apart along layers, but close together in the direction normal to the layering. This creates zones, depicted in the centre panel of Figure 1, which are very anisotropic in strongly layered locations, and which extend along the reflectors. Points in less coherent areas tend to have zones which are smaller and nearly isotropic, so they are more clustered and less patterned.

A comparison between traditional inversion methods and the presented IGT method is demonstrated in Figure 2. The top panel shows a stacked image overlaid with a velocity update from an inversion process with traditional Laplacian regularization, without dip-guiding or other structure-constraint methods. The centre panel is similar, but with simple dip-guided Laplacian regularization. This update more closely follows structure seen in highly dipping locations, but demonstrates little improvement in resolution or overall quality. The bottom panel shows the velocity update for the same input data, with the inversion conditioned by the IGI constraint. This IGT update tends to be much more strongly constrained to the layers observed in the stacked image, and it demonstrates a noticeably higher resolution. Layers are more distinctly separated from their neighbours, particularly in the shallow regions which have a very low resolution update with more traditional approaches, and the deeper areas follow the strong dips seen in the stacked image much more closely.

Figure 3 shows a three-dimensional representation of the stacked image used to guide inversion results, and the corresponding IGT velocity update. The update is very closely tied in each direction to the structure observed in the image.

Offset-dependent picking

Polynomial-based RMO picking methods are effective when events demonstrate smooth curvature coinciding with low order polynomial terms, and significant improvements have been made by industrial institutes to improve this technique in real data processing (He and Cai, 2011; Bartana et al., 2011; Siliqi et al., 2007; Koren et al., 2008). However, problems arise when the real curvature shows greater complexity, and the polynomial assumption may be inaccurate (Liu et al., 2010). Events with multiple turning points may arise in a variety of situations, particularly near faults, in areas with high anisotropy, and in strongly heterogeneous regions. For these events, flattening the near offsets may lead to worse fits at far offsets, or vice versa, and determining the best pick will mean sacrificing accuracy at some offset ranges. As an alternative to polynomial-based methods, and due to the increasing demand for high-resolution imaging, offset-dependent techniques, such as the plane-wave destruction method described by Fomel (2002; Liu et al., 2010), have gained attention in the past decade. By picking the RMO at all available offsets, we may ensure that complex moveout is being appropriately considered in tomographic updates, which in turn will cause updates to converge more quickly to a model which effectively flattens events.

In our offset-dependent picking method, the RMO is represented as a continuous displacement field rather than a series of discrete events. A multi-scale, constrained solver is used to estimate the displacement field for each common image gather. The principal constraint applied is that the gradient of the displacement field g is less than some tolerance T, where T is less than 1 (Hale, 2013), or

$$|\nabla_z g(h, z) < T, \qquad (3)$$

where h and z represent the offset and depth of each point in an offset gather, respectively. This constraint prevents waveform distortion caused by excessive stretching and squeezing, as well as picks which cross one another. The events with maximum coherence are then computed from the derived displacement field. The advantage of this approach is that the computed events will be more consistent than if each event is estimated independently. This is important as exploration moves to increasingly complex targets in subsalt, sub-basalt, and other deep prospect regions, where gathers are likely to be highly complicated and contaminated by noise.

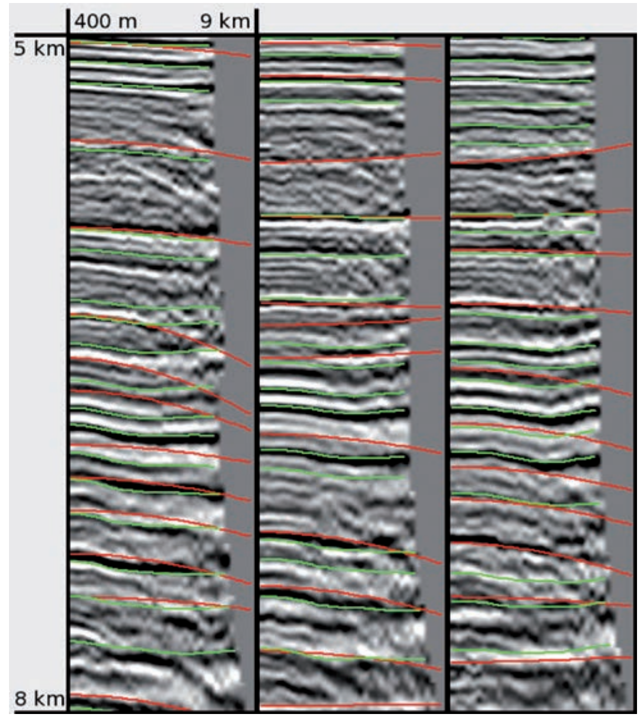

Figure 4 *Cotton Valley Formation example. Pre-stack depth migration gathers overlaid with RMO picks selected by (green) offset-dependent picking and (red) hyperbolic picking.*

This new picking method is very effective for areas displaying good signal-to-noise. However, for poor signal-to-noise regions, careful quality control is needed to avoid picking wrong events, such as multiples. Once picks are calculated, the tomographic process continues with the typical tasks of ray tracing and inversion, making this update fit easily into the existing workflow.

Offset-dependent picking example

Figures 4 to 8 follow a case study which was conducted on a region showing complicated stack and gather behaviour, providing an ideal demonstration of the capabilities of offset-dependent picking.

The region of interest in this case is the Cotton Valley Formation (CVF) layer within the Gulf of Mexico's Lloyd Ridge area. The CVF is a layer of shale with carbonate stringers which shows very little coherent reflectivity to tie to events. Gathers depict complex moveout beneath the CVF layer corresponding to undulations in stacked images which conventional hyperbolic picking was unable to resolve. Figure 4 compares hyperbolic picks in red to offset-dependent picks in green. Clearly, updating velocity based on hyperbolic picks will, at best, solve issues over a small offset range, and, at worst, make events significantly less flat. However, after an iteration of tomography using offset-dependent picking, gather flatness is increased even for complex events, as shown in Figure 5. The most dramatic changes, as expected, are seen below the CVF, represented by the blue bracket on each pair of gathers.

As can be seen in Figure 6, the stacked image before the offset-dependent update appears geologically plausible above the CVF, which extends from about 5.7 to 6.4 km as shown by the blue bracket. Below this incoherent layer, reflectors display unphysical undulations and kinks, pointed out by the blue arrows. The overlaid velocity model, which is only shown along the CVF, is clearly too smooth at this time to reflect the strongly heterogeneous velocity changes which must be present to fix this issue. Figure 7 then shows a stacked image after an offset-dependent update, also overlaid with this new velocity model. The undulations observed in the previous image below the CVF layer, are greatly reduced, leading to more coherent and plausible layering, which coincides with increased flatness in the gather events. It is also interesting to note that details in the velocity model now correspond well with small features in the stacked image, expected to be embedded carbonate stringers, suggesting that this method is allowing us to resolve small inhomogeneities in the physical make-up of the CVF layer.

Depth slices through the CVF, shown in Figure 8, help to emphasize that the updates generated using offset-dependent picking tend to reflect the complicated geology of the region better than more simplistic picking methods. Before this iteration of tomography, the velocity model is very smooth and does not follow image trends, as shown in the top panel. A new velocity model, gained by updating with hyperbolic picking, is shown in the centre panel. While the resolution is increased by this process, the update does not seem to encourage the model to more closely tie to the area's geology. However, the new model obtained with an offset-dependent update, shown in the bottom panel, displays features which much more accurately reflect the complicated heterogeneous structures observed in the image. Strong reflections arise at the interface between the shale and carbonate stringers, which should also separate high

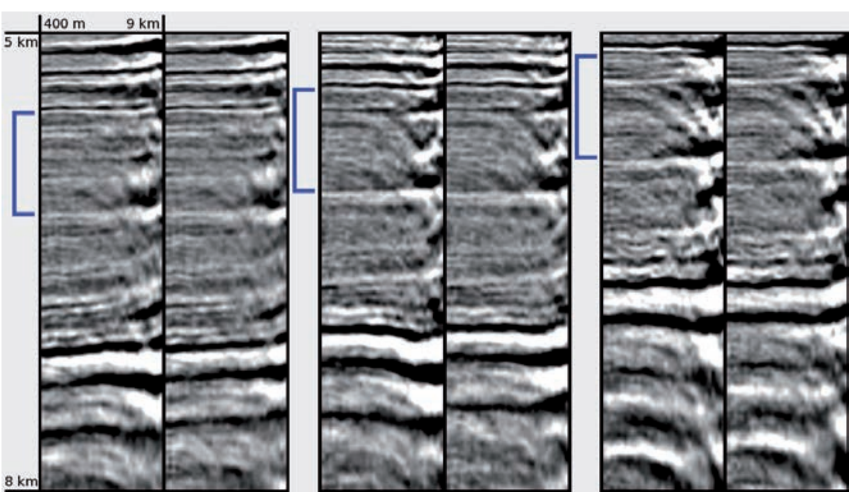

***Figure 5** Cotton Valley Formation example. Three pairs of gathers before (left gather of each pair) and after (right) an iteration of offset-dependent tomography. The approximate position of the CVF layer in each pair of gathers is indicated by the blue bracket.*

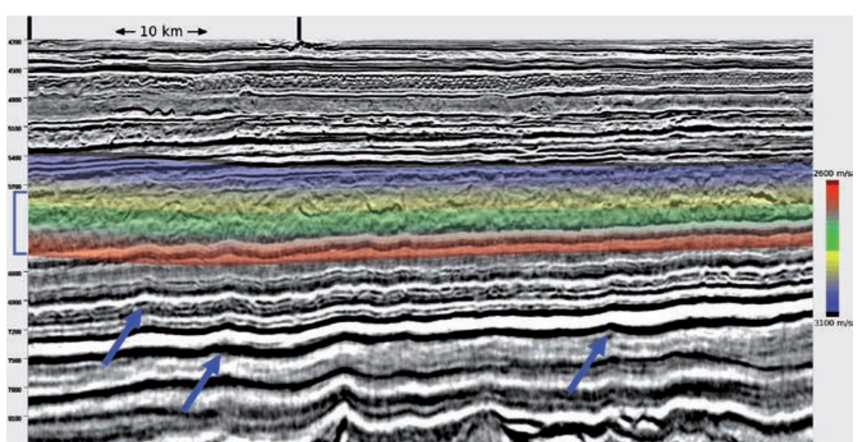

***Figure 6** Cotton Valley Formation example. Stacked image before offset-dependent tomography overlaid with the current smooth velocity model, highlighting the CVF layer of interest, which is also pointed out by the blue bracket. Blue arrows indicate undulations which are flattened significantly in Figure 7.*

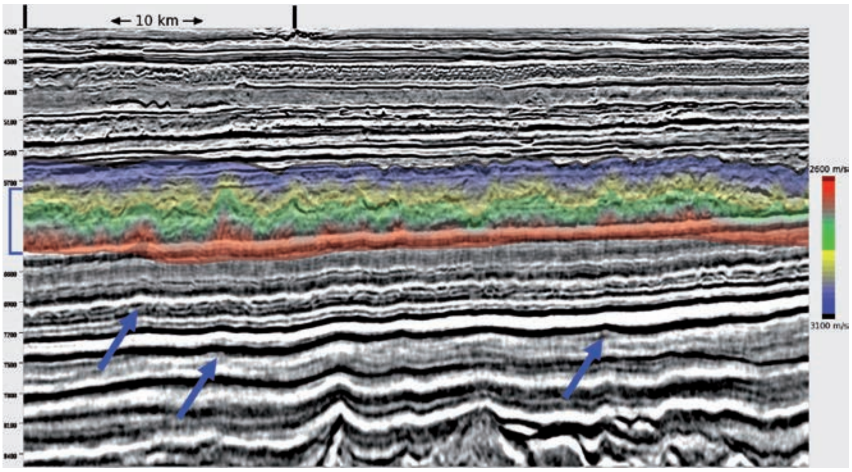

Figure 7 *Cotton Valley Formation example. Stacked image after an iteration of offset-dependent tomography, overlaid with the updated velocity model, which clearly ties to the complicated events observed in the CVF layer, shown with the blue bracket. Blue arrows point out undulations which are greatly improved from Figure 6.*

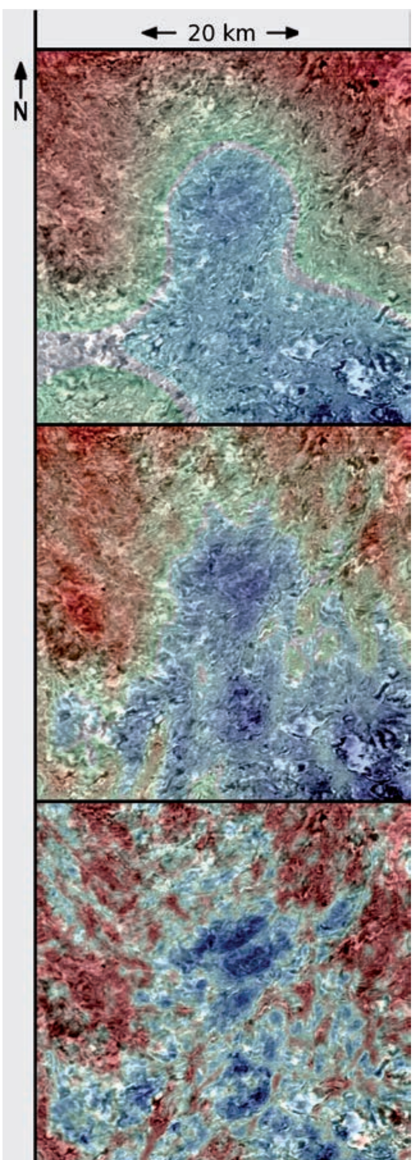

Figure 8 *Cotton Valley Formation example. Velocity model overlaid on stacked image depth slice at 6 km (top panel) before update, (centre panel) after one tomographic iteration using hyperbolic picking, and alternatively, (bottom panel) after one iteration using offset-dependent picking. All three panels are shown with the same color bar.*

and low velocity zones, and the new picking method clearly honours this distinction more effectively.

Overall, the velocity updates obtained using offset-dependent picking lead to models, gathers, and, most importantly, images, which more accurately reflect the geology of the complicated CVF region.

Conclusions

While conventional tomographic methods can often adequately flatten gathers, advanced approaches to improve accuracy and likelihood can both speed up the convergence of velocity models, and generate more geologically plausible models.

Appropriate conditioning of the inversion scheme leads to better results than more simplistic methods. With traditional inversion schemes, tomographic velocity updating is a purely mathematical process, and therefore does not tend to provide updates which respect the observed subsurface structure. Image-guided tomography uses an edge-preserving structure-oriented preconditioner that encourages updates to follow structure, leading to more geologically plausible higher resolution velocity models which honour layering and faults automatically. The Angola example demonstrates clearly that image-guided tomography can produce results which show much greater resolution, strong adherence to layering and faults, and fewer artefacts than conventional tomographic approaches.

Upgrading from curvature-based residual moveout picking to an offset-dependent scheme can allow more precise description of complex events to yield more accurate velocity updates without relying on ineffective assumptions on their nature. Gather events which display multiple turning points or do not span the entire offset range, which would previously be incorrectly picked, are well-fit and appropriately flattened. In the Gulf of Mexico dataset presented, a single iteration of tomography with offset-dependent picking is able to resolve complicated inhomogeneities in the disorganized Cotton Valley Formation layer, improving gather flatness and stacked image layering.

Our high-resolution tomography suite combines these methods into a new tomography flow, melding easily with earlier techniques. New results are a vast improvement over those obtained with conventional methods, yielding more accurate velocity models, and frequently saving computation time and effort.

Acknowledgments
The authors would like to thank TGS for permission to use the examples contained within. We also thank Alex Yeh, Bin Wang, Jean Ji, Cristina Reta-Tang, and Gary Rodriguez for valuable contributions, discussion, and support of this work. Special gratitude is owed to Zhiming Li, Connie VanSchuyver, Chris Egger, and Jeff Sposato for reviewing and proofreading this article.

References

Bartana, A., Kosloff, D. and Hollander, Y. [2011] Automatic picking of delays on 3D angle gathers. *SEG Annual Meeting*, Expanded Abstracts, 3903-3907.

Cullison, A. [2011] An image-guided method for automatically picking common-image-point gather locations from seismic images. *CWP Thesis* 702.

Fomel, S. [2002] Applications of plane-wave destruction filters. *Geophysics*, **67**(6), 1946–1960.

Hale, D. [2009a] Image-guided blended neighbour interpolation. *CWP Report* 634.

Hale, D. [2009b] Structure-oriented smoothing and semblance. *CWP Report* 635.

Hale, D. [2013] Dynamic warping of seismic images. *Geophysics*, **78** (2).

He, Y. and Cai, J. [2011] Anisotropic tomography for TTI and VTI media. *SEG Annual Meeting*, Expanded Abstracts, 3923-3927.

Koren, Z., Ravve, I., Gonzalez, G. and Kosloff, D. [2008]. Anisotropic local tomography. *Geophysics*, **73**(5), VE75–VE92.

Liu, J. and Han, W. [2010] Automatic event picking and tomography on 3D RTM angle gathers. *SEG Annual Meeting*, Expanded Abstracts, 4263–4268.

Siliqi, R., Herrmann, P., Prescott, A. and Capar, L. [2007] High-order RMO picking using uncorrelated parameters. *SEG Annual Meeting*, Expanded Abstracts, 2772-2776.

Woodward, M., Nichols, D., Zdraveva, O., Whitfield, P. and Johns, T. [2008] A decade of tomography. *Geophysics*, **73**, 5–11.